XPD Enhancement of Dipole Antenna Arrays by Inducing Coherent Current From Feeding Line

Xiao Tan, Xide Mei, and Ke-Li Wu, *Fellow, IEEE*

***Abstract*— Cross-polarization discrimination (XPD) is a critical parameter in designing dual-polarized antennas, particularly for multiple-input–multiple-output (MIMO) base station (BS) antenna arrays. A high XPD level leads to high isolation between two polarized waves and a high input signal-to-noise ratio of the system. In this article, a new scheme for enhancing XPD of a ±45° dual-polarized dipole antenna pair, the most prevalent antenna element form for MIMO BS antenna arrays, is proposed and is applied to a dipole antenna array. The new scheme induces the required coherent currents on a pair of vertical monopoles from the feeding line. Specifically, a 3-U structure that is printed on the circuit board of the feeding line is proposed. The structure couples the signal from the feeding line and excites two opposite currents on the vertical monopoles, whose radiated fields effectively compensate the θ-component of electric field in a wide scanning angle. The working principle of the scheme is elaborated in detail with a simplified analytic model. The scheme is applied to a dipole array, in which each 3-U structure is personally designed to accommodate the complex array environment. Simulation and experimental results are presented to demonstrate the effectiveness of the proposed scheme.**

***Index Terms*— Antenna arrays, antenna radiation patterns, cross-polarization discrimination (XPD), dipole antennas, multiple-input–multiple-output (MIMO).**

I. Introduction

The multiple-input–multiple-output (MIMO) technology has become the most prevalent spatial multiplexing scheme in modern wireless communication systems. The massive MIMO (M-MIMO) systems that comprise large-scale antenna arrays at base stations (BSs) can significantly enhance the spatial multiplexing gain, energy efficiency, and spectral efficiency [1], [2], [3], [4], [5], [6]. While gaining the favorable benefits, M-MIMO systems also face many challenges in the physical layer. As far as the M-MIMO array antenna is concerned, the eminent challenges facing the designers include the strong mutual couplings among antenna elements, the distortion of element radiation patterns, and the poor cross-polarization discrimination (XPD) at wide scanning angles.

XPD is a critical parameter for a pair of antennas polarized perpendicularly in ±45° with respect to the horizon. Such an antenna pair can be a pair of linearly polarized antenna elements or two independent beamforming antenna arrays. XPD measures the isolation between two perpendicularly polarized channel signals, in dB. A poor XPD indicates a significant degradation in the signal-to-noise ratio of the system at the antenna end where the interference from the other polarization channel is unbearable. Antenna elements with ±45° dual polarizations are commonly adopted in antenna arrays for BSs in sub-6-GHz bands to minimize the multipath fading effect and to improve the received signal quality [7]. The relationship between XPD and channel performance has been well investigated in [8], which states that the higher the XPD level of a ±45°dual-polarized antenna pair is, the higher the channel throughput.

Many efforts have been paid to suppress the cross polarization of a single antenna in the past. In [9], a double-layered vertical printed dipole antenna is proposed with low cross-polarization (X-pol) by suppressing the transversal components of E-field. However, the method is not suitable for a horizontal printed dipole antenna. In [10], two T-shaped slots are cut in a dual-polarized patch antenna to achieve a low cross-polarized wave. In [11], [12], and [13], a symmetrical structure with a differential feeding method is adopted to achieve a low X-pol slot antenna. In [14], a meander-line ring cavity is introduced to suppress the X-pol of a circularly polarized microstrip antenna. However, the traditional schemes for X-pol suppression are not applicable for XPD enhancement of a ±45°dual-polarized antenna pair since enhancing XPD is more than suppressing X-pol. It requires a good balance of the θ- and ϕ-components of the electric field within a wide off-boresight angle. A lower X-pol does not necessarily imply a higher XPD for a ±45° dual-polarized antenna pair. In recent years, some efforts have been made on XPD enhancement of ±45° dual-polarized antenna pairs. In [15], a circular loop that is shorted through via pins is placed around a dual-polarized dipole antenna pair for XPD enhancement. In [16], four horizontal parasitic elements are placed around a dual-polarized dipole antenna pair along a square contour with an edge length of about one wavelength for XPD enhancement. A common problem facing the methods in [14], [15], and [16] is their excessively required space, which is difficult to have in a compact M-MIMO antenna array. In [17],

Manuscript received 21 July 2022; revised 6 February 2023; accepted 14 February 2023. Date of publication 24 March 2023; date of current version 5 May 2023. This work was supported in part by the Postgraduate Scholarship of The Chinese University of Hong Kong and in part by the Research Funding from Huawei Technologies Company on antenna array technologies. *(Corresponding author: Ke-Li Wu.)*

The authors are with the Department of Electronic Engineering, The Chinese University of Hong Kong, Hong Kong (e-mail: xtan@link.cuhk.edu.hk; xdmei@link.cuhk.edu.hk; klwu@ee.cuhk.edu.hk).

Color versions of one or more figures in this article are available at https://doi.org/10.1109/TAP.2023.3256304.

Digital Object Identifier 10.1109/TAP.2023.3256304

a dual-layered loop antenna is proposed, which combines both electric and magnetic currents to achieve a better phase balance to enhance XPD. However, only phase compensation is achieved, lacking control of magnitude compensation of the θ-component of the electric field, which limits the flexibility of XPD enhancement. Nevertheless, among the aforementioned approaches, none accommodates the need to improve the XPD of a dual-polarized antenna pair in an MIMO antenna array, for which the induced currents on each antenna element for compensating the E-field in a wide scanning angle need to be controlled individually with a high degree of freedom.

Enhancing XPD of an antenna array is usually much more difficult than a single dual-polarized antenna pair, especially for an array requiring a wide scanning angle. This is because the typical environment of an antenna pair in an array is different from each other due to different scattering effects of the surrounding and the secondary radiation of the coupled signal to the neighboring antennas, which also contribute to the total radiation. As a result, antenna pairs at different positions in an array will encounter different XPD conditions. Such an XPD personality in designing a high-performance antenna array must be dealt with preferably using an agile, simple, and self-contained passive structure with sufficient design freedom. A typical specification for XPD of an MIMO antenna array is about 18 dB in the boresight direction and 8 dB at $\pm 60^\circ$ despite difficulties. Usually, the XPD in a wide scanning angle is much more difficult to control. This article presents an attempt on this difficult issue.

In this article, a new scheme for enhancing XPD of a pair of $\pm 45^\circ$ dual-polarized dipole antenna, which is the most common antenna form for an MIMO antenna array, is introduced. The scheme induces the required coherent currents on a pair of vertical monopoles on the two opposite edges of each antenna from the feeding line. Specifically, a triple-U (3-U) shaped passive structure that is printed on the vertical circuit board of the feeding line is proposed with its application to an M-MIMO antenna array. An approximated analytic model is presented to illustrate the working principle of the 3-U structure for XPD enhancement. Both EM simulation and experimental results justify the feasibility of the scheme and the effectiveness of the proposed structure. To apply the 3-U structure to a dipole antenna array, the personalized radiation characteristic of each individual dipole antenna pair is sketched by perturbing multiple physical design parameters of the 3-U structure. The basic concept of the new scheme is to introduce coherent secondary radiation from the two outmost vertical segments of the 3-U structure in a controlled manner. The additional radiation enhances the θ-component of E-field in the off-boresight directions, leading to a higher XPD within a wide scanning angle. Compared to the existing XPD enhancement approaches, the proposed 3-U structure exhibits the following unique and attractive attributes.

1) The secondary coherent radiation from the 3-U structure is naturally immune to the surrounding as the secondary current is induced directly from the feeding line rather than by the radiated field, which can be easily perturbed by the environment.
2) Being printed on the same substrate as the feeding line, the 3-U structure is compact and cost-free.
3) With multiple dimensional controlling variables, the induced coherent current for the secondary radiation can be easily tuned in a wide range of magnitude and phase to accommodate the complex environments in an antenna array.

Although only a 3×3 uniform dipole antenna array operating in the frequency band of 1.7–1.9 GHz is theoretically and experimentally investigated in this article, it is asserted that the structure can be applied to a wide range of uniform or staggered dipole antenna arrays for M-MIMO system applications.

II. XPD Enhancement of a Single Dipole Antenna Pair

In this section, the 3-U structure for XPD enhancement of a dual-polarized dipole antenna pair is introduced. The working principle is explained by an analytical model. Simulation and experimental results are provided to demonstrate the effectiveness of this method. A parametric study is conducted with regard to several important design parameters.

A. Antenna and 3-U Configurations

Without loss of generality, a pair of $\pm 45^\circ$ dual-polarized dipole antennas operating in 1.7–1.9 GHz is considered as the illustration example. The configuration of the antenna pair with 3-U structure is shown in Fig. 1(a)–(c), in which two orthogonal eight-shaped dipole arms are printed on the bottom layer of the horizontal substrate that is supported by two vertically crossed substrates oriented in $\pm 45^\circ$. The vertical supporting substrates are about quarter a wavelength high and are also used as the substrates for microstrip feeding lines of the two dipoles. Typical feeding structures for such crossed dipole antennas include coaxial line [10], [16], differential feed [15], and balun [9], [17]. The feeding structure adopted in this design is a feeding pad connected to the microstrip feedline. It crosses over two dipole arms and serves as a balun. To reduce the size of the radiating arms, two vertically bended wings at the ends of each dipole antenna are also printed on the supporting substrates. Two sets of three U-shaped metal strips, whose opening mouths face up and down alternatively, are printed on the same side as the feeding lines on the two separate supporting substrates. Note that the three U-shaped strips are not completely backed by the ground plane, leaving the two outmost vertical arms ungrounded for radiating. Each U strip is about but less than half a wavelength long to avoid resonance in the working frequency band. As shown in Fig. 1(d) and (e), the coherent signals on the two outmost U strips are coupled from the two sides of the feeding line, one of which is coupled through the middle U strip such that the phases of the currents on the two outmost vertical arms are opposite. It will be shown that the 3-U structure can provide high flexibility to adjust the amount of the coupled signals from the feeding line of the corresponding dipole antenna. In the illustrative example, the substrates are with a dielectric constant of 4.4 and a thickness of 0.8 mm. Other detailed dimensions are listed in Table I.

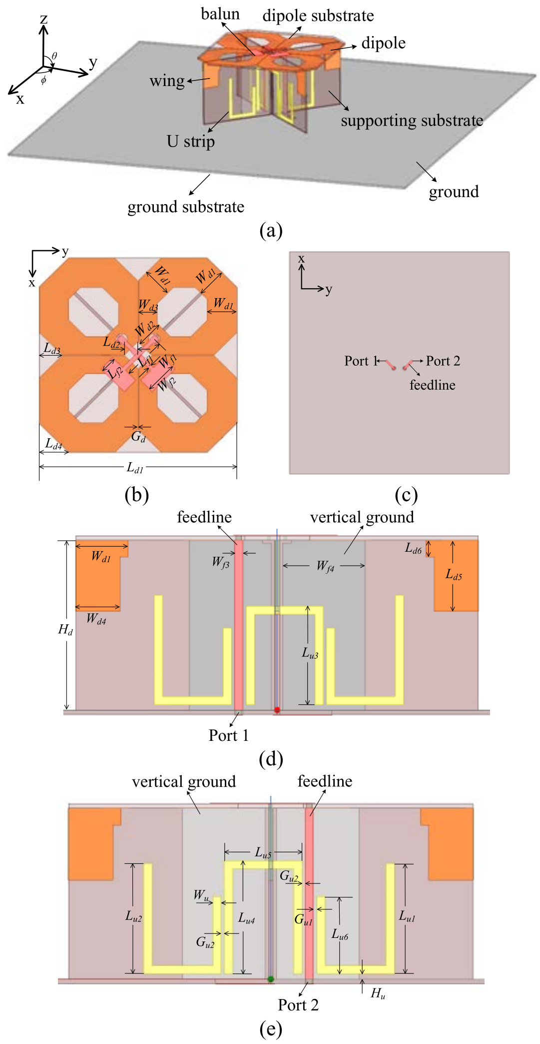

Fig. 1. Configuration of the ±45° dual-polarized dipole antenna pair with the 3-U structure: (a) perspective view, (b) top view of the dipole antennas, (c) bottom view of the substrate for the dipole antennas, (d) view on the plane of $\phi = 45°$, and (e) view on the plane of $\phi = 135°$.

TABLE I
DIMENSIONS OF THE DIPOLE ANTENNA PAIR WITH THE 3-U STRUCTURE (MM)

L_{d1}	L_{d2}	L_{d3}	L_{d4}	L_{d5}	L_{d6}	G_d
60	4	6	8.3	13	3	0.2
W_{d1}	W_{d2}	W_{d3}	W_{d4}	L_{f1}	L_{f2}	H_d
9.5	8	5.7	8	12.9	5	31
W_{f1}	W_{f2}	W_{f3}	W_{f4}	W_u	G_{u1}	G_{u2}
1.2	9.2	1.5	15	1.5	0.6	0.6
L_{u1}	L_{u2}	L_{u3}	L_{u4}	L_{u5}	L_{u6}	H_u
20	20	18	20.5	14	14	1

B. Working Principle of the 3-U Structure

XPD is defined as the ratio of the E-field component in the co-polarization (C-pol) to that in X-pol of one antenna element in a ±45° dual-polarized antenna pair. As shown in Fig. 2, when the 45° polarized antenna is excited, the E-field components in the C-pol $[E_C(\theta)]$ and X-pol $[E_X(\theta)]$ directions in the xoz plane ($\phi = 0°$) can be found by the projection of

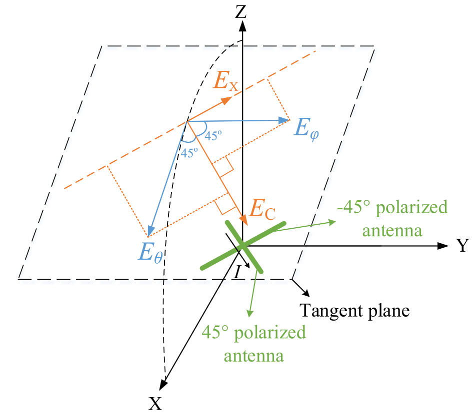

Fig. 2. Illustration of C-pol and X-pol for a 45° polarized antenna.

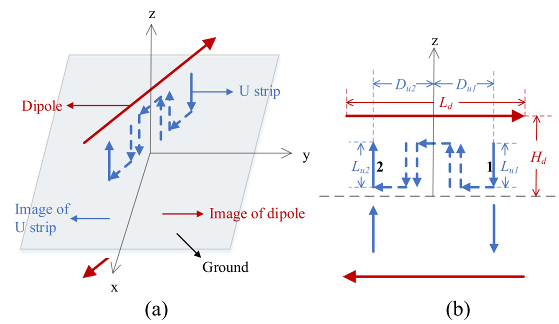

Fig. 3. Current distributions of a simplified dipole antenna with the 3-U structure in (a) perspective view and (b) view on the plane of $\phi = 135°$. Solid arrow: radiating segments. Dashed arrow: nonradiating segments.

E_θ and E_ϕ in the tangent plane as

$$E_C(\theta) = E_\phi(\theta)\cos 45° + E_\theta(\theta)\cos 45°$$
$$E_X(\theta) = E_\phi(\theta)\sin 45° - E_\theta(\theta)\sin 45°. \quad (1)$$

The XPD in the xoz plane ($\phi = 0°$) is defined by

$$\text{XPD}(\theta) = \frac{E_C(\theta)}{E_X(\theta)} = \frac{E_\phi(\theta) + E_\theta(\theta)}{E_\phi(\theta) - E_\theta(\theta)}. \quad (2)$$

Note that the X-pol component of the 45° polarized antenna is exactly the C-pol component of the −45° polarized antenna and vice versa, that is to say, XPD describes the ratio of the signal in one of a ±45° dual-polarized antenna pair versus that of the other one in the far field. It can be observed that XPD will theoretically approach infinity as the denominator $E_\phi(\theta) - E_\theta(\theta)$ approaches zero. This quantity is dimensionless and is usually expressed in a logarithmic scale (dB).

In order to analytically investigate the XPD issue of a pair of dipole antennas, the current distribution on a dipole in the simplified wire antenna model is assumed to be piecewisely sinusoidal with both ends open-circuited. The outmost vertical arms of the 3-U structure are considered as two vertical monopoles above the ground plane. The directions of the currents are indicated by arrows in Fig. 3. Referring to Fig. 1(e), currents are coupled from the feedline to the two adjacent U strips and are further coupled to the third U strip through the middle U strip. The magnitude of the currents can be controlled by the length of each U strip and the gaps between U strips. It can be observed from the EM simulation that the two out-of-phase vertical currents are generated on the two outmost vertical arms, which are the main contributors to the XPD enhancement. Other current segments on the 3-U structure (dashed arrows) have little influence on the radiation due to the vertical ground plane on the back. In the analytical analysis, the magnitude and phase of each current component are suggested by the HFSS EM simulation. The image currents due to the horizontal ground plane are also considered.

Consider a $-45°$ polarized ideal dipole antenna, as shown in Fig. 3(a). The total E-field of the simplified model can be found by the superposition of the fields contributed by each individual current segment, including the radiating segments of the 3-U structure. The dimensions for the simplified model are labeled in Fig. 3(b). The magnitude maximum of the piecewise sinusoidal current on the dipole antenna is assumed to be I_d. The two outmost vertical arms of 3-U, namely, arms 1 and 2, with their image currents, are considered as vertical dipoles with piecewise sinusoidal current distribution with magnitude maximum of I_{u1} and I_{u2}, respectively. The phasor form of the E-field radiated by the dipole antenna together with its image in the far field in the plane of $\phi = 0°$ can be found as [18]

$$E_{\theta,d}(\theta) = j\eta \frac{I_d e^{-jkr}}{2\sqrt{2}\pi r}\left[\frac{\cos\left(\frac{kL_d}{2\sqrt{2}}\sin\theta\right) - \cos\left(\frac{kL_d}{2}\right)}{\left(1-\frac{1}{2}\sin^2\theta\right)}\right] \cdot \cos\theta\left(e^{jkH_d\cos\theta} - e^{-jkH_d\cos\theta}\right) \quad (3)$$

$$E_{\phi,d}(\theta) = -j\eta \frac{I_d e^{-jkr}}{2\sqrt{2}\pi r}\left[\frac{\cos\left(\frac{kL_d}{2\sqrt{2}}\sin\theta\right) - \cos\left(\frac{kL_d}{2}\right)}{\left(1-\frac{1}{2}\sin^2\theta\right)}\right] \cdot \left(e^{jkH_d\cos\theta} - e^{-jkH_d\cos\theta}\right) \quad (4)$$

where L_d is the length of the dipole antenna, H_d is the height of the dipole antenna above the ground plane, r is the distance of the observation point to the origin, η is the wave impedance, and k is the wavenumber. On the other hand, the aggregated phasor form of the E-field radiated by the two outmost vertical arms with their images only contributes to the $E_\theta(\theta)$ component and can be found as

$$\begin{aligned} E_{\theta,u}(\theta) &= j\eta \frac{I_{u1}e^{-jkr}}{2\pi r}\left[\frac{\cos(kL_{u1}\cos\theta) - \cos(kL_{u1})}{\sin\theta}\right] e^{jk\frac{D_{u1}}{\sqrt{2}}\sin\theta} \\ &\quad - j\eta \frac{I_{u2}e^{-jkr}}{2\pi r}\left[\frac{\cos(kL_{u2}\cos\theta) - \cos(kL_{u2})}{\sin\theta}\right] e^{-jk\frac{D_{u2}}{\sqrt{2}}\sin\theta} \end{aligned} \quad (5)$$

where L_{u1} and L_{u2} are the lengths of vertical arms 1 and 2, respectively, and D_{u1} and D_{u2} are the distances of arms 1 and 2 to the z-axis. According to (2), the XPD of this $-45°$ polarized antenna will approach infinity when $E_\phi(\theta) = -E_\theta(\theta)$. It can be observed from (3) and (4) that $E_{\phi,d}$ and $E_{\theta,d}$ are exactly out of phase, but their magnitudes are differed by $(1 - \cos\theta)$, which increases as θ increases. The role of the 3-U structure is to compensate the E_θ component of the dipole antenna and to reduce the discrepancy between E_θ and E_ϕ. For an ideal dipole antenna, the two arms of the 3-U should be symmetrical such that $I_{u1} = I_{u2}$, $L_{u1} = L_{u2}$, and $D_{u1} = D_{u2}$, in order for $E_{\theta,u}$ to be in phase with $E_{\theta,d}$.

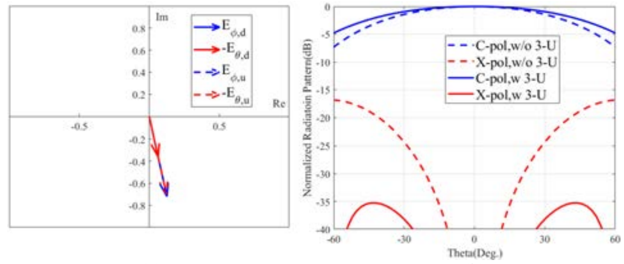

(a) (b)

Fig. 4. E-field compensation in the plane of $\phi = 0°$ analyzed by the simplified analytic model: (a) normalized phasor diagram of E_θ and E_φ by dipole antenna and the 3-U with $\theta = 60°$ (or $\theta = -60°$) and (b) normalized radiation pattern with (solid lines) and without (dashed lines) 3-U structure for $\theta \in [-60°, 60°]$.

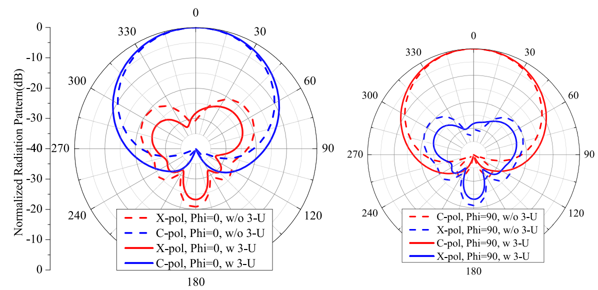

(a) (b)

Fig. 5. EM-simulated normalized radiation patterns of the dipole antenna pair with (solid lines) and without (dashed lines) the 3-U structure at 1.8 GHz in the plane of (a) $\phi = 0°$ and (b) $\phi = 90°$ when port 2 is excited.

When a high XPD is required for $\theta \in [-60°, 60°]$, the E-field compensation condition at $\theta = \pm 60°$ needs to be examined. As shown in Fig. 4(a), in which the arrows represent the E-field phasors that comprise normalized magnitude and phase information, $-E_{\theta,d}$ (the red solid line arrow) has the same phase as that of $E_{\phi,d}$ (the blue solid line arrow) but with a smaller magnitude. In the plots, the initial phase is not important and is arbitrarily chosen. It is also shown that with the compensation of $E_{\theta,u}$ (the red dashed line arrow) contributed by the 3-U, the total $-E_\theta$ and E_ϕ reaches a good balance, leading to, as shown in Fig. 4(b), an enhanced XPD over a wide range of angles. To plot the phasor diagram in Fig. 4(a), the E-field radiated by the 3-U structure cannot be directly obtained but can be obtained by subtracting the E-field radiated by the antenna alone from the E-field radiated by the antenna with the 3-U structure. The phasor diagrams for $\theta = -60°$ and $\theta = 60°$ are the same due to the symmetry of the E-field. It is also noted from Fig. 4(b) that the compensation of the $E_{\theta,u}$ component also increases the boresight beamwidth, which will slightly lower the antenna gain.

C. Experimental Validation

A dual-polarized dipole antenna pair with the proposed 3-U structure is EM designed, prototyped, and experimentally investigated. The EM-simulated normalized radiation patterns of the dipole antenna pair with and without the 3-U structure at 1.8 GHz when port 2 is excited are compared in Fig. 5. It can be seen that XPD is enhanced by about 5–6 dB for $\theta = \pm 60°$with the 3-U structure applied.

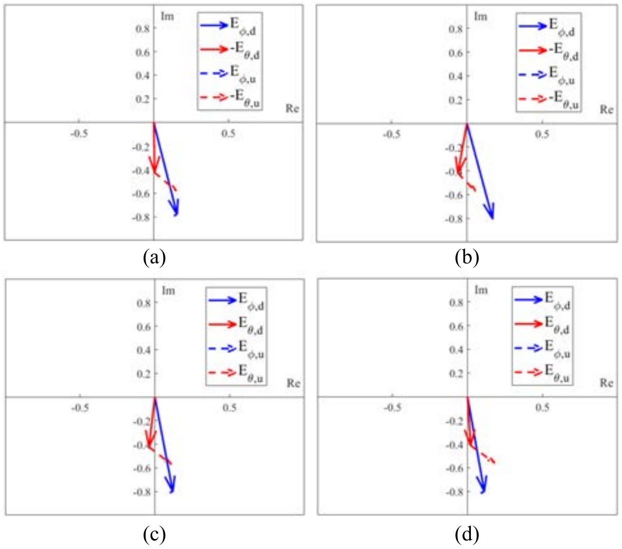

Fig. 6. EM-simulated normalized phasor diagrams of E_θ and E_φ for the dipole antenna and the 3-U structure at 1.8 GHz when port 2 is excited: (a) $\phi = 0°$ and $\theta = -60°$, (b) $\phi = 0°$ and $\theta = 60°$, (c) $\phi = 90°$ and $\theta = -60°$, and (d) $\phi = 90°$ and $\theta = 60°$.

To validate the working principle explained by the approximate wire antenna model, the E-field vector diagrams of the EM-simulated dipole antenna and those of the 3-U structure at $\theta = \pm 60°$ are plotted in Fig. 6. Similar to the analysis of the simplified model in Fig. 4(a), with the compensation of $E_{\theta,u}$ contributed by the 3-U, the total of $-E_\theta$ and E_ϕ are closer to each other, resulting in the enhanced XPD. The vectors of the EM-simulated $E_{\phi,u}$ component are negligibly small to be noticed, as expected.

The EM designed ±45° dual-polarized dipole antenna pairs with and without the 3-U are fabricated and the measured S-parameters are shown in Fig. 7. The matching condition may be affected slightly due to a small amount of signals coupled from the feeding line. A slight deviation in matching can be adjusted by fine-tuning the dimensions of the antenna. The measured normalized radiation patterns at 1.7, 1.8, and 1.9 GHz, with and without the 3-U when port 2 is excited are compared in Fig. 8, showing obviously the enhanced XPD of 5~7 dB at $\theta = \pm 60°$ at the center frequency of 1.8 GHz and justifying the analytic model. Enhancements of XPD at 1.7 and 1.9 GHz are also obvious. The proposed 3-U structure is not a wideband structure due to its resonating nature (each U structure is a half-wavelength resonator). Nevertheless, a variety of wideband coupler circuits can be applied for wideband dipole antennas with the same concept. It is worth mentioning that the measured total gains of the antenna pairs with and without the 3-U are 8.81 and 9.28 dBi with almost the same measured total efficiency of about 92% at 1.8 GHz. The 0.47-dB gain loss is due to the additional C-pol E-field component contributed by the 3-U that broadens the beamwidth and reduces the directivity.

D. Parametric Study

According to (5), the E-field radiated by the 3-U structure is mainly affected by the magnitude and phase of currents, the lengths, and the positions of the two outmost vertical arms. The magnitudes of the currents depend on the length of each U strip. Hereby, parametric studies are conducted on the vertical length L_{u1} and L_{u2} and horizontal length L_{u5} by HFSS EM simulation, as shown in Figs. 9–11. The phasor $E_{\theta,u}$ rotates clockwise with increased magnitude as L_{u5} increases. The current magnitude increases as the length of the U strip increases. The phase variation of E_θ component occurs due to the imperfect symmetry of the 3-U structure with respect to the vertical central line of the dipole antenna.

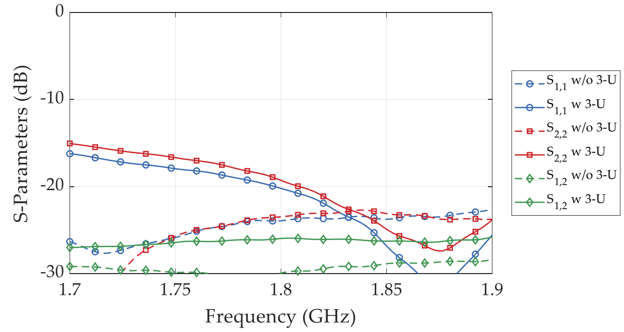

Fig. 7. Measured S-parameters of the dipole antenna pair with (solid lines) and without (dashed lines) the 3-U structure.

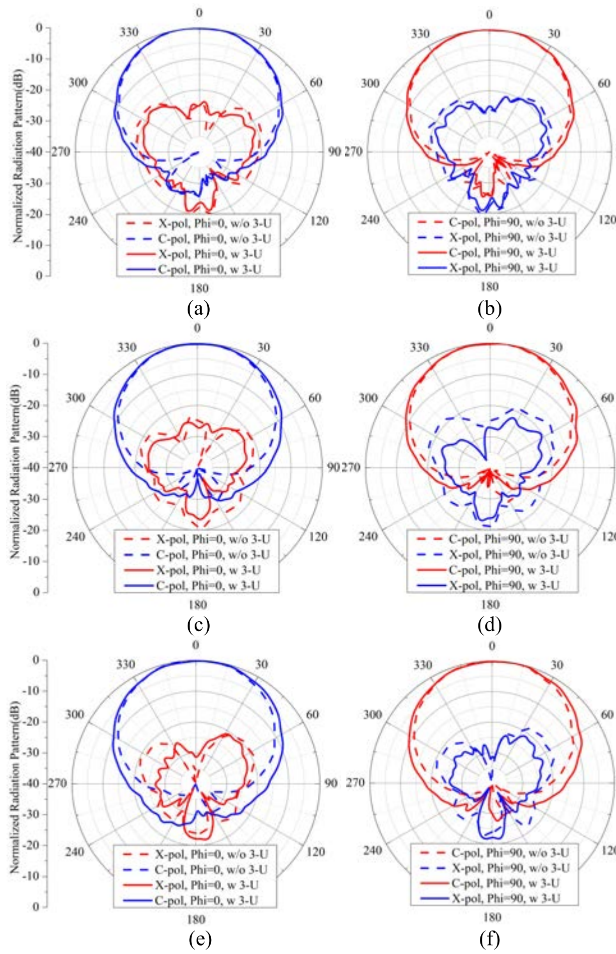

Fig. 8. Measured normalized radiation patterns of the dipole antenna pair with (solid lines) and without (dashed lines) the 3-U structure with port 2 excited at (a) and (b) 1.7 GHz, (c) and (d) 1.8 GHz, and (e) and (f) 1.9 GHz in the planes of $\phi = 0°$ and $\phi = 90°$.

As L_{u1} or L_{u2} increases, the phase variations in $\pm\theta$ angles in the plane of either $\phi = 0°$ or $\phi = 90°$ are different, which allows relatively independent control of XPD in $\pm\theta$ angles. It can be observed that the effects of L_{u1} and L_{u2} complement each other. The parametric study provides a clear guideline for personalized design of the 3-U structure on each dual-polarized dipole antenna pair in a dipole antenna array for overall XPD enhancement.

III. XPD Enhancement of a Dipole Antenna Array

Having shown the design guideline, it will be demonstrated that the proposed 3-U structure can be individually applied to each antenna element in a dipole antenna array for overall XPD enhancement.

A. XPD Issues in a Dipole Array

Dealing with the XPD problem in an array is much more challenging than that of a standalone dual-polarized antenna pair due to the complex surrounding environments in an array. First, there is a strong scattering effect that perturbs the near field. Second, the induced current on surrounding antenna elements also contributes to the far field. Therefore, the 3-U structure for different antenna elements requires different personalized designs.

To demonstrate this point, a 3 × 3 uniform array that uses the dual-polarized dipole antenna pair shown in Fig. 1 is considered. The array configuration and element numbering are shown in Fig. 12 with a spacing of 0.64 and 0.47 λ in the x- and y-directions, respectively. The EM-simulated normalized radiation patterns of the dipoles at the center (dipole 10) and edge (dipole 2) of the array are plotted in Fig. 13(a) and (b), respectively. Compared to the radiation pattern of a standalone dipole antenna pair without the 3-U structure shown in Fig. 5, it can be observed that the XPD of a dipole pair in an array environment is deteriorated significantly in most of the angles for $\theta \in [-60°, 60°]$. The XPDs of the dipole antennas at the center and edge of the array behave very differently, of which the XPD of the center dipole pair is impaired most. Therefore, the 3-U structures for the center and edge elements in an array need to be designed individually.

B. Personalized Design for Antenna Elements in an Array

The 3-U structure is applied to all the antenna elements in the array individually with different dimensions. The following design procedure is suggested:

1) applying a unified 3-U design with proper dimensions to all the antenna elements first;
2) obtaining phasor diagrams of the E-field of each antenna element and fine-tuning the 3-U design for each element individually according to the rule of thumb observed in the parametric study;
3) reiterating step 2) based on the updated phasor diagrams of the E-field until a satisfactory result is achieved.

According to the Cannikin law, if the original XPD is sufficiently good, there is no need for additional enhancement as the poorest XPD in the scanning angles determines the system performance. As XPD is a strong function of the observation angle, an optimal design must be taken holistically.

In this demonstration example, typical antenna elements (with port numbers 2, 4, 8, and 10) with distinct array environments are chosen to illustrate the performance. Following the design procedure, the final dimensions of the

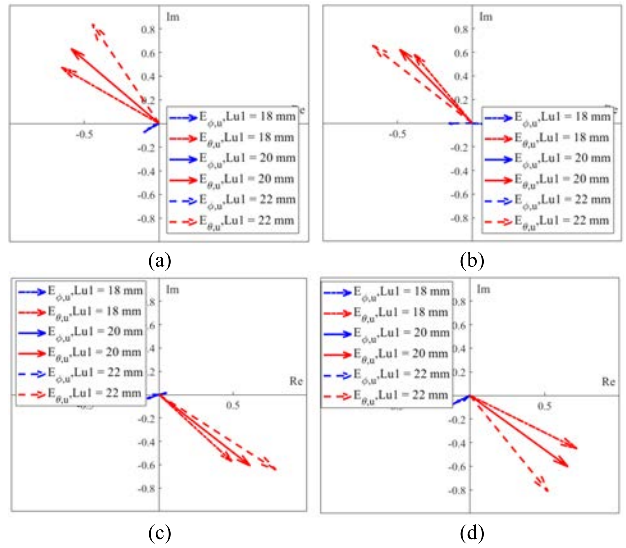

Fig. 9. Parametric study of $Lu1$ on normalized E-field components of the 3-U structure: (a) $\phi = 0°$ and $\theta = -60°$, (b) $\phi = 0°$ and $\theta = 60°$, (c) $\phi = 90°$ and $\theta = -60°$, and (d) $\phi = 90°$ and $\theta = 60°$.

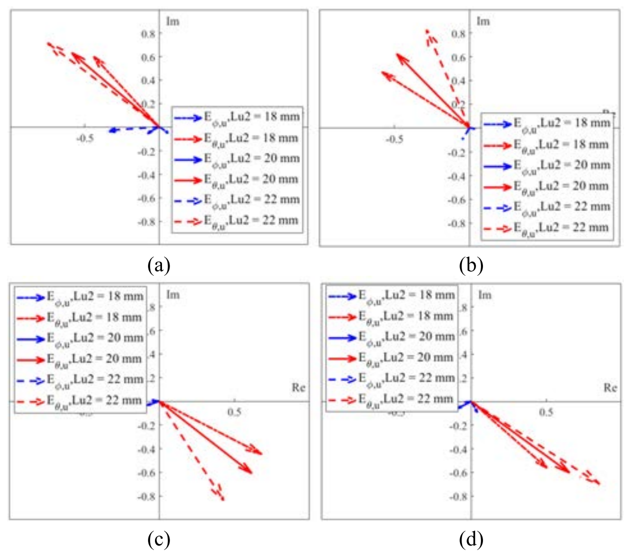

Fig. 10. Parametric study of L_{u2} on normalized E-field components of the 3-U structure: (a) $\phi = 0°$ and $\theta = -60°$, (b) $\phi = 0°$ and $\theta = 60°$, (c) $\phi = 90°$ and $\theta = -60°$, and (d) $\phi = 90°$ and $\theta = 60°$.

TABLE II
Dimensions of the Dipole Antenna With Individual 3-U Structure in the Array (mm)

	L_{d3}	L_{d6}	W_{d1}	L_{u1}	L_{u2}	L_{u5}
Port 2	5.5	5	9	20	19	14
Port 4				21	19	14
Port 8				21	21	13
Port 10				20	19	14

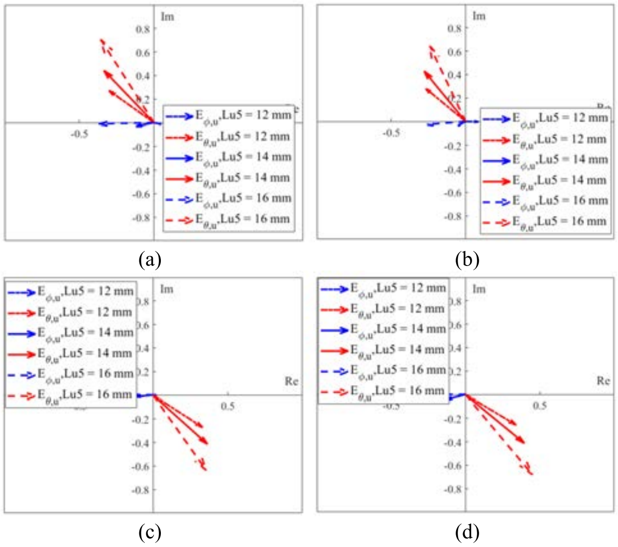

Fig. 11. Parametric study of L_{u5} on normalized E-field components of the 3-U structure: (a) $\phi = 0°$ and $\theta = -60°$, (b) $\phi = 0°$ and $\theta = 60°$, (c) $\phi = 90°$ and $\theta = -60°$, and (d) $\phi = 90°$ and $\theta = 60°$.

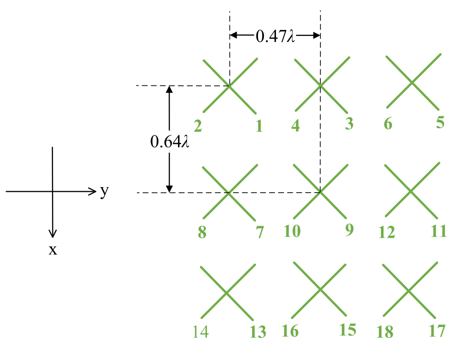

Fig. 12. Configuration of the 3 × 3 uniform dipole antenna array and element numbering scheme.

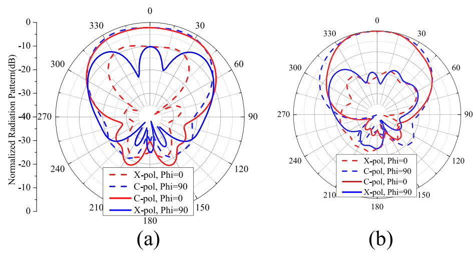

Fig. 13. EM-simulated normalized radiation patterns of typical elements in the array at 1.8 GHz: (a) center element dipole 10 and (b) edge element dipole 2.

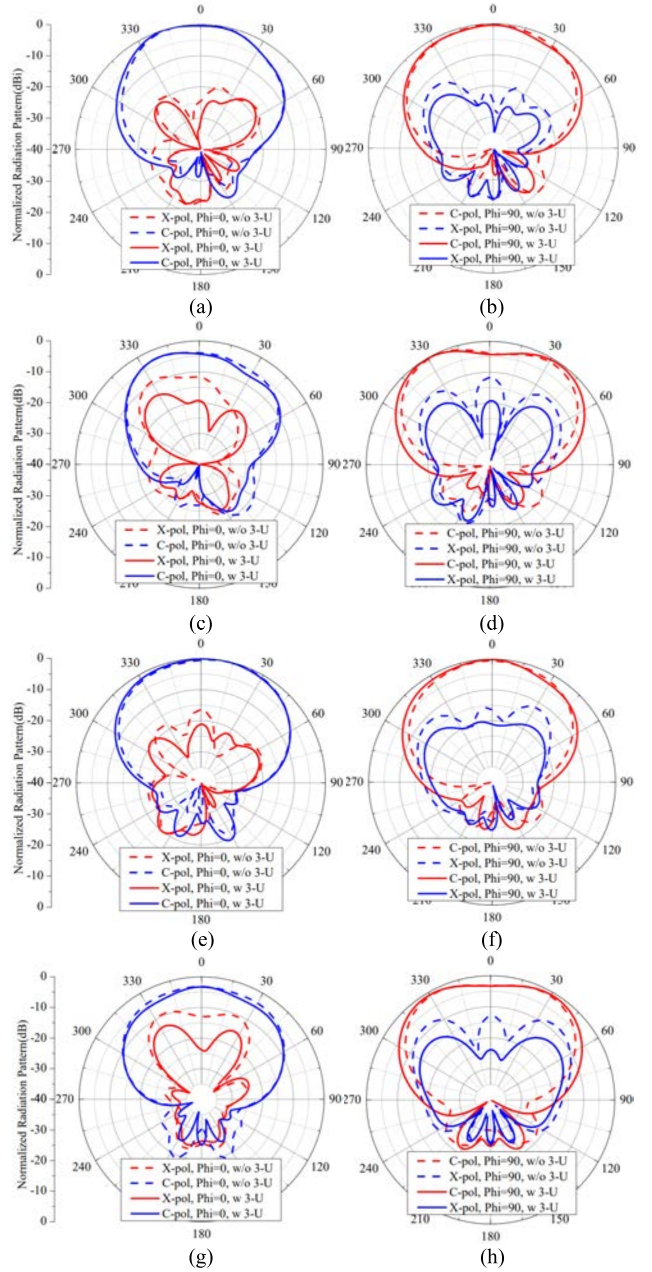

Fig. 14. EM-simulated normalized radiation patterns of the dipole array with (solid lines) and without (dashed lines) using the 3-U structure at 1.8 GHz: (a) and (b) port 2 excited, (c) and (d) port 4 excited, (e) and (f) port 8 excited, and (g) and (h) port 10 excited in the planes of $\phi = 0°$ and $\phi = 90°$.

3-U structures of the chosen antenna elements as well as some dimensional adjustments of dipole antenna pairs in the array can be obtained, as listed in Table II. All the other dimensions of antenna elements not listed in Table II are the same as those of the standalone dipole antenna pair, as listed in Table I. The EM-simulated normalized radiation patterns of the typical antenna elements with and without using the 3-U structure at 1.8 GHz are compared in Fig. 14, showing obvious enhancement in XPD at most of the angles for most of the cases when the 3-U structure is applied except those angles at which original XPD is already sufficiently high (say, greater than 15 dB) and does not deterministically affect the system performance.

The 3 × 3 uniform dipole array with individually designed 3-U structures is fabricated. The photograph of the prototyped antenna array is shown in Fig. 15 with the element numbering scheme shown in Fig. 12. The measured S-parameters of typical elements of the dipole array with and without using the 3-U structure in the frequency band of 1.7–1.9 GHz are compared in Fig. 16. It can be observed that all the matching conditions are improved and most of the mutual couplings are reduced after applying the 3-U structure. The measured normalized radiation patterns of the typical antenna elements

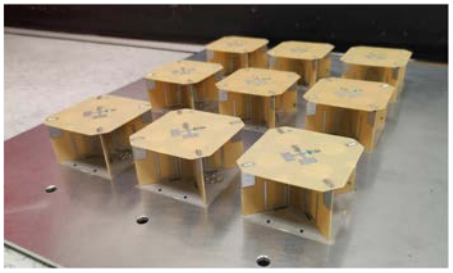

Fig. 15. Photograph of the fabricated 3 × 3 uniform dipole array with the 3-U structure.

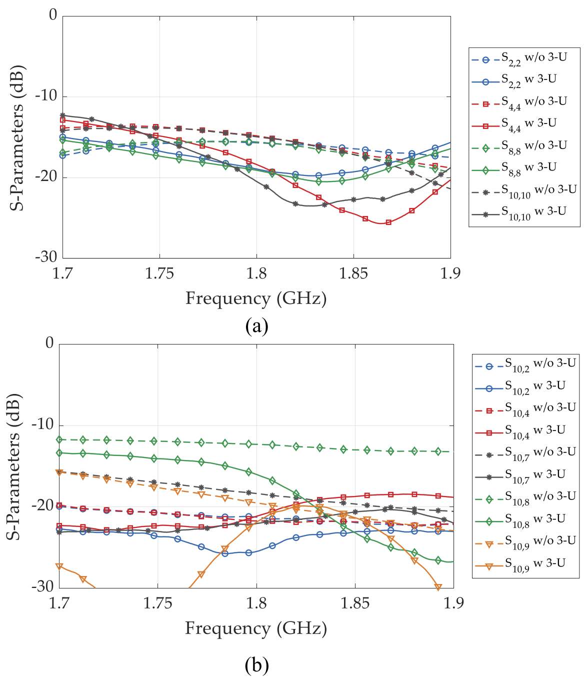

Fig. 16. Measured (a) reflection coefficients of typical antenna elements and (b) typical mutual couplings of the 3 × 3 uniform dipole array with (solid lines) and without (dashed lines) using the 3-U structure.

TABLE III
COMPARISON WITH OTHER XPD ENHANCEMENT SCHEMES

Reference	[15]	[16]	[17]	This work
Poorest XPD at $\theta = \pm 60°$ (dB)	10.9	12	10.5	12.9
Overall size (λ_0)	1.03	1.03	0.45	0.36
Applicability to array	No	No	No	Yes

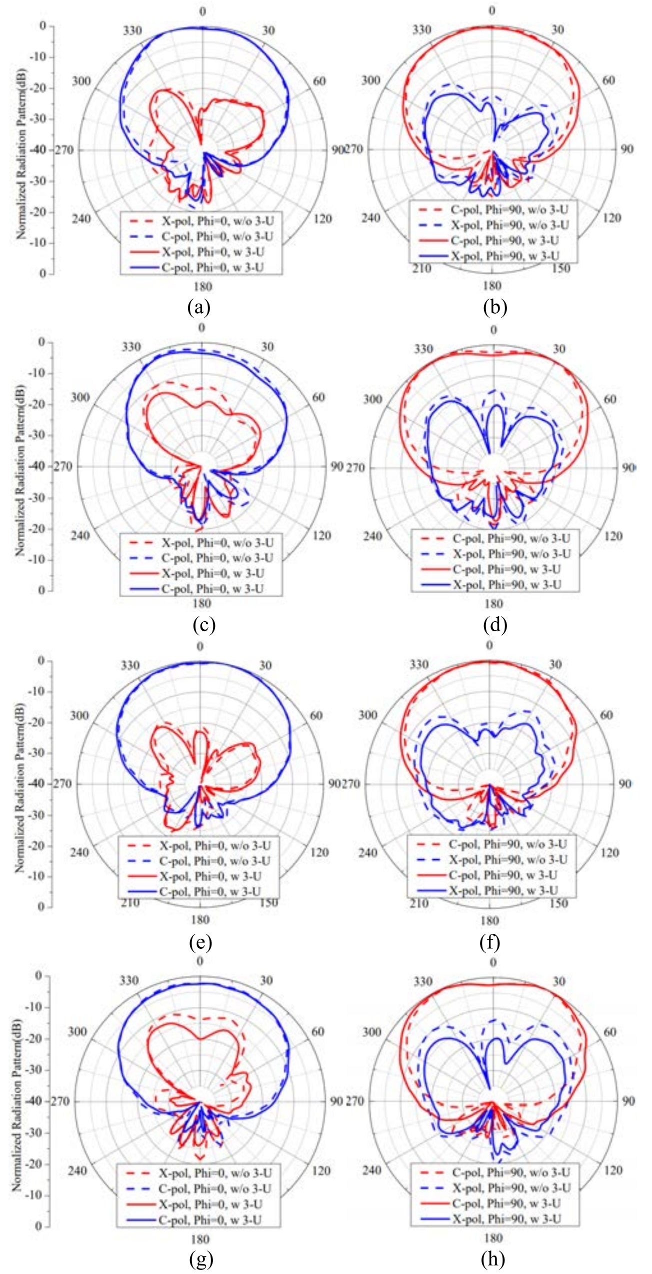

Fig. 17. Measured normalized radiation patterns of the dipole array with (solid lines) and without (dashed lines) using the 3-U structure at 1.8 GHz: (a) and (b) port 2 excited, (c) and (d) port 4 excited, (e) and (f) port 8 excited, and (g) and (h) port 10 excited in $\phi = 0°$ and $\phi = 90°$ planes, respectively.

(ports 2, 4, 8, and 10) in the dipole antenna array with and without the 3-U structure at 1.8 GHz are compared in Fig. 17. Similar to the EM-simulated results, the measured XPD is enhanced at most of the angles for the cases where the original XPDs are poor. Noticeably, the XPD of element 10 at $\theta = -60°$ and $+60°$ in the $\phi = 90°$ plane is enhanced from 4.38 to 9.1 dB and from 3.37 to 8.3 dB, respectively. The overall XPD improvement demonstrates that the 3-U structure is effective for XPD enhancement of a two-dimensional dual-polarized dipole antenna array.

In summary, the proposed XPD enhancement scheme is a viable option to improve the overall XPD of a practical dipole antenna array. Table III presents a comparison of the proposed 3-U structure with the XPD enhancement schemes in [15] and [17]. The horizontal edge dimension in terms of the wavelength at the center frequency of the antenna pair is used to gauge the antenna element size. The poorest XPD of a standalone antenna pair at $\theta = \pm 60°$ in the planes of $\phi = 0°$ and 90° at the center frequency is compared to show the effectiveness of the enhancement, although the metrics can not reflect the unique ability that enhances the very poor XPD of a dipole antenna pair in an array environment. Considering the practical limit of the maximum dimension of an antenna element and that no additional space is required for XPD enhancement, the proposed XPD enhancement scheme is shown to be the most viable technique for ±45° dual-polarized dipole antenna arrays.

IV. Conclusion

In this article, a new scheme for enhancing XPD of a ±45° dual-polarized dipole antenna pair and the array is proposed by introducing appropriate coherent currents from the feeding line. A specific realization of the scheme is a novel antenna auxiliary structure with three U-shaped strips or the 3-U structure. The structure supplements the required θ-component of the E-field of a pair of dual-polarized dipole antennas in a wide off-boresight angle by the radiated field from the 3-U structure, leading to enhanced XPD. Compared to existing XPD enhancement schemes, the proposed 3-U structure has exhibited many unique and attractive attributes, including the most compact size, high immunity from the surrounding environment, which is critical to its use in a two-dimensional antenna array, multiple design variables, and no additional cost. The working principle and design concept of the 3-U structure are well explained by an analytical approximate wire antenna model. In addition to theoretical and experimental investigation of a standalone dual-polarized antenna pair, the proposed 3-U structure is also applied to a 3 × 3 uniform dipole antenna array, for which each 3-U structure is individually designed to accommodate different array environments of each antenna element, showing significant overall XPD enhancement. This work is the first attempt to address the XPD issue in a ±45° dual-polarized two-dimensional dipole antenna array. It is expected that the proposed 3-U structure can be used in designing high-performance M-MIMO antenna arrays for BSs of 5G and future wireless communication systems.

References

[1] M. Giordani, M. Polese, M. Mezzavilla, S. Rangan, and M. Zorzi, "Toward 6G networks: Use cases and technologies," *IEEE Commun. Mag.*, vol. 58, no. 3, pp. 55–61, Mar. 2020.

[2] M. Farasat, D. N. Thalakotuna, Z. Hu, and Y. Yang, "A review on 5G sub-6 GHz base station antenna design challenges," *Electronics*, vol. 10, no. 16, p. 2000, Aug. 2021.

[3] S. Yang and L. Hanzo, "Fifty years of MIMO detection: The road to large-scale MIMOs," *IEEE Commun. Surveys Tuts.*, vol. 17, no. 4, pp. 1941–1988, 4th Quart., 2015.

[4] C. D. Ho, H. Q. Ngo, M. Matthaiou, and T. Q. Duong, "On the performance of zero-forcing processing in multi-way massive MIMO relay networks," *IEEE Commun. Lett.*, vol. 21, no. 4, pp. 849–852, Apr. 2017.

[5] N. V. Deshpande, S. Dey, D. N. Amudala, and R. Budhiraja, "Spatially-correlated IRS-aided multiuser FD mMIMO systems: Analysis and optimization," *IEEE Trans. Commun.*, vol. 70, no. 6, pp. 3879–3896, Jun. 2022.

[6] H. Q. Ngo, E. G. Larsson, and T. L. Marzetta, "Energy and spectral efficiency of very large multiuser MIMO systems," *IEEE Trans. Commun.*, vol. 61, no. 4, pp. 1436–1449, Apr. 2013.

[7] R. G. Vaughan, "Polarization diversity in mobile communications," *IEEE Trans. Veh. Technol.*, vol. 39, no. 3, pp. 177–186, Aug. 1990.

[8] Y.-G. Lim, Y. J. Cho, T. Oh, Y. Lee, and C.-B. Chae, "Relationship between cross-polarization discrimination (XPD) and spatial correlation in indoor small-cell MIMO systems," *IEEE Wireless Commun. Lett.*, vol. 7, no. 4, pp. 654–657, Aug. 2018.

[9] Z. Zhou, S. Yang, and Z. Nie, "A novel broadband printed dipole antenna with low cross-polarization," *IEEE Trans. Antennas Propag.*, vol. 55, no. 11, pp. 3091–3093, Nov. 2007.

[10] B. Li, Y.-Z. Yin, W. Hu, Y. Ding, and Y. Zhao, "Wideband dual-polarized patch antenna with low cross polarization and high isolation," *IEEE Antennas Wireless Propag. Lett.*, vol. 11, pp. 427–430, 2012.

[11] H. Qi and H. Liu, "Single-ended band-notched vivaldi antenna with common mode suppression and low cross polarization," *IEEE Antennas Wireless Propag. Lett.*, vol. 20, no. 10, pp. 1983–1987, Oct. 2021.

[12] C. Chen, C. Li, Z. Zhu, and W. Wu, "Wideband and low-cross-polarization planar annual ring slot antenna," *IEEE Antennas Wireless Propag. Lett.*, vol. 16, pp. 3009–3013, 2017.

[13] T. Oh, Y.-G. Lim, C.-B. Chae, and Y. Lee, "Dual-polarization slot antenna with high cross-polarization discrimination for indoor small-cell mimo systems," *IEEE Antennas Wireless Propag. Lett.*, vol. 14, pp. 374–377, 2014.

[14] X. Chen, D. Wu, L. Yang, and G. Fu, "Compact circularly polarized microstrip antenna with cross-polarization suppression at low-elevation angle," *IEEE Antennas Wireless Propag. Lett.*, vol. 16, pp. 258–261, 2016.

[15] Z. Tang, J. Liu, and Y. Yin, "Enhanced cross-polarization discrimination of wideband differentially fed dual-polarized antenna via a shorting loop," *IEEE Antennas Wireless Propag. Lett.*, vol. 17, no. 8, pp. 1454–1458, Aug. 2018.

[16] Y. Luo, Q.-X. Chu, and D.-L. Wen, "A plus/minus 45 degree dual-polarized base-station antenna with enhanced cross-polarization discrimination via addition of four parasitic elements placed in a square contour," *IEEE Trans. Antennas Propag.*, vol. 64, no. 4, pp. 1514–1519, Apr. 2016.

[17] C. Ding, H.-H. Sun, R. W. Ziolkowski, and Y. J. Guo, "A dual layered loop array antenna for base stations with enhanced cross-polarization discrimination," *IEEE Trans. Antennas Propag.*, vol. 66, no. 12, pp. 6975–6985, Dec. 2018.

[18] C. A. Balanis, *Antenna Theory: Analysis and Design*, 3rd ed. Hoboken, NJ, USA: Wiley, 2005, pp. 133–144.

Xiao Tan received the B.Eng. degree in electronic engineering from The Chinese University of Hong Kong, Hong Kong, in 2018, where she is currently pursuing the Ph.D. degree in electronic engineering.

Her current research interests include decoupling and XPD enhancement of MIMO antenna arrays and filtering antenna design for BS applications.

Xide Mei received the B.S. degree in electronic engineering from the University of Electronic Science and Technology of China, Chengdu, China, in 2015, and the Ph.D. degree in electronic engineering from The Chinese University of Hong Kong, Hong Kong, in 2022.

His current research interests include protocol stack development, physical layer development, core network development, and system integration for RAN.

Ke-Li Wu (Fellow, IEEE) received the B.S. and M.Eng. degrees from the Nanjing University of Science and Technology, Nanjing, China, in 1982 and 1985, respectively, and the Ph.D. degree from Laval University, Quebec, QC, Canada, in 1989.

From 1989 to 1993, he was a Research Engineer with McMaster University, Hamilton, ON, Canada. He joined COM DEV (now Honeywell Aerospace), Cambridge, ON, Canada, in 1993, where he was a Principal Member of Technical Staff. Since 1999, he has been with The Chinese University of Hong Kong, Hong Kong, where he is currently a Professor and the Director of the Radio frequency Radiation Research Laboratory. His current research interests include theory and practical problems in microwave filters, MIMO antenna arrays, and IoT technologies.

Prof. Wu is a member of the IEEE MTT-S TC5 Committee. He was a recipient of the 1998 COM DEV Achievement Award and the Asia–Pacific Microwave Conference Prize twice in 2008 and 2012.